Single-Chain Folding Nanoparticles as Carbon Nanotube Catchers

Mesut Bilgi,[1] Demet Karaca Balta,[1] Binnur Aydogan Temel ,[2] Gokhan Temel [3]

[1]Department of Chemistry, Yildiz Technical University, Istanbul 34220, Turkey
[2]Department of Pharmaceutical Chemistry, Faculty of Pharmacy, Bezmialem Vakif University, Fatih, Istanbul 34093, Turkey
[3]Department of Polymer Engineering, Faculty of Engineering,Yalova University, Yalova 77200, Turkey
Correspondence to: G. Temel (E-mail: gtemel@yalova.edu.tr)

Received 26 June 2018; Accepted 10 September 2018; published online 17 October 2018
DOI: 10.1002/pola.29245

ABSTRACT: This contribution describes a simple method for preparing polymeric nanoparticles using photodimerization of anthracene moieties on the side chain of terpolymers in dilute regime and transformation of obtained polymeric nanoparticles into pyrene functional nanoparticles via Menschutkin quaternization procedure. Subsequently, pyrene possessing polymeric nanoparticles are attached onto multiwalled carbon nanotube (MWCNT) surfaces by π–π stacking strategy. Gel permeation chromatography, thermal gravimetric analysis, ultraviolet–visible, and fluorescence spectroscopies are used to analyze modified nanoparticles and their precursors. Electron microscopy and dispersion studies show that pyrene-modified polymeric nanoparticles are able to interconnect various CNTs. © 2018 Wiley Periodicals, Inc. J. Polym. Sci., Part A: Polym. Chem. **2018**, *56*, 2709–2714

KEYWORDS: carbon nanotube; hybrid materials; photodimerization; polymeric nanoparticles

INTRODUCTION The development of the intramolecular chain folding has been a field of polymer science and technology because of its crucial potential applications on CO_2 capturing,[1] production of catalysis,[2–4] drug delivery,[5] and responsive polymeric materials.[6–8] Chain folding process is one of the most unique and reliable method to produce functional macromolecular nanoparticles. Linear precursor undergoes intramolecular chemical interactions in dilute condition and transforms into the folded-chain structure. Resulting polymeric nanostructure becomes a more compact particle and generally it is smaller than its previous size. Crosslinkable species can be located on the side chains of the linear precursor by varying chemical techniques or added externally to the reaction environment in order to synthesize polymeric nanoparticles.[9–11] Therefore, several synthetic strategies have been carried out to achieve nanosized materials such as photodimerization,[12–14] stepwise folding,[15] benzocyclobutene chemistry,[16] and atom transfer radical coupling.[17,18]

After discovery of carbon nanotubes (CNTs) in 1991, polymer science has found a new pathway for nanotechnology applications like drug delivery systems,[19] microelectronics,[20,21] energy storage,[22] and biotechnology.[23] Although CNTs have major drawbacks such as self-aggregation, lack of solubility in conventional solvents and low dispersion behavior in polymer matrix due to the strong van der Waals forces between particles, they include powerful properties such as low mass density, electrical and thermal conductivity, high aspect ratio, chemical stability under harsh conditions, and nanocomposite component.[24] In order to overcome these disadvantages, noncovalent and covalent functionalization methodologies were addressed in various publications and modified CNTs were successfully achieved with improved dispersion properties.[24–30] Noncovalent route is extensively applied to obtain modified nanostructures such as π–π stacking interactions between CNT walls and polynuclear aromatic group containing polymers. The use of noncovalent technique is an efficient way to achieve functional CNTs without alteration of their intrinsic behaviors such as molecular conjugation, optical, and thermal properties.[31–34]

In order to obtain the benefits of both polymeric nanoparticle and CNT, we decorated surface of CNT with single-chain folding polymeric nanoparticles (SCNPs) via noncovalent interactions strategy. First, amine and anthracene containing terpolymer was readily synthesized by radical polymerization technique. Afterward, polymeric nanoparticles were achieved by dimerization of anthracene moieties on the side chain of the terpolymers in dilute medium and pyrene functional nanoparticles were achieved via straightforward Menschutkin quaternization procedure using tertiary amine functionalities of nanoparticles and 1-(bromoacetyl)pyrene. Finally, pyrene possessing polymeric nanoparticles were attached onto

Additional supporting information may be found in the online version of this article.

multiwalled carbon nanotube (MWCNT) surfaces using π–π stacking interactions.

EXPERIMENTAL

Materials

α,α′-Azoisobutyronitrile (AIBN, 98%) was purchased from Aldrich (Germany) and recrystallized from ethanol. MWCNT Baytubes C 150 P (Bayer, Germany), *N*,*N*-dimethylformamide (DMF, Merck, Germany), methanol (Merck, Germany), *n*-hexane (Merck, Germany), 1-(bromoacetyl)pyrene (Aldrich, 97%, Germany), 9-anthracenemethanol (Aldrich, 97%, Germany), tetrahydrofuran (THF, Sigma-Aldrich, 99.9%, contains BHT as inhibitor, Germany), and methacryloyl chloride (97%, contains ~200 ppm monomethyl ether hydroquinone as stabilizer, Aldrich, Germany) were used as received. Methyl methacrylate (MMA, Aldrich, 99%, Germany) and 2-(diethylamino)ethyl methacrylate (contains 1500 ppm MEHQ as inhibitor, DEAEMA, Aldrich, 99%, Germany) were deinhibited by passing over basic alumina. All other reagents were used as received.

Instrumentation

A merry-go-round type photoreactor (Kerman) equipped with 18 Philips 8W lamps emitting light nominally at λ = 350 nm was used. Ultraviolet (UV) spectra were recorded on Hitachi U-2900. Fluorescence emission spectra were recorded on Hitachi F-2700 spectrophotometer. Proton nuclear magnetic resonance (^{1}H NMR) spectra were performed on a Bruker Avance Spectrometer (500 MHz) using $CDCl_3$ as solvent. Gel permeation chromatography (GPC) measurements were performed on a Viscotek GPCmax VE 2001 Autosampler system equipped with Viscotek VE 3580 refractive index (RI) detector. Three Viscotek GPC columns (T3000, LT4000L, and LT5000L), (7.8 mm internal diameter, 300 mm length), and a Viscotek guard column (CLM3008, 4.6 mm internal diameter, 10 mm length) were used in series. The effective molecular weight ranges were 456–42,800, 1050–107,000, and 10,200–2,890,000, respectively. THF was used as an eluent at a flow rate of 1.0 mL min^{-1} at 35 °C. Detector was calibrated with polystyrene (PS) standards having narrow molecular weight distribution. Data were analyzed using Viscotek OmniSEC 4.7.0 software. Particle size distributions were determined using dynamic light scattering (DLS) in THF dispersions using a Malvern NanoZSP instrument. Differential scanning calorimetry (DSC) measurements were performed on a TA Instruments DSC-Q200 with a heating rate of 10 °C min^{-1} under nitrogen atmosphere. TGA measurements were carried out with a SEIKO ExStar 6300 instrument under inert atmosphere at a heating rate of 10 °C min^{-1} between 25 and 850 °C. The morphology of nanostructures was analyzed by a high-resolution transmission electron microscope (HRTEM) JEOL JEM-2100 and samples were prepared by drop coating a dilute solution of the sample in THF on a holey carbon-coated copper grid.

Synthesis of Methacrylated Anthracene

Methacrylated anthracene (AntMac) was synthesized according to a modified literature procedure.[12] Synthetic procedure was carried out as follows: methacryloyl chloride (0.75 mL, 7.5 mmol) dissolved in THF (1.5 mL) was added dropwise to a solution of 9-anthracenemethanol (1.04 g, 5 mmol) and triethylamine (0.7 mL, 5 mmol) in the mixture of THF (20 mL) at 0 °C under nitrogen atmosphere. After the addition of methacryloyl chloride solution, the resulting mixture was stirred at room temperature overnight in the dark. After addition of 30 mL dichloromethane, the mixture was washed with excess water and saturated aqueous solution of $NaHCO_3$ (200 mL). To neutralize the organic phase, extraction was carried out with saturated aqueous solution of NaCl (200 mL). The organic layers were dried over anhydrous Na_2SO_4, filtered, and then the solvent was evaporated. The resulting residue was purified by recrystallization from methanol. Yield: 65%. Gas chromatography–mass spectrometry (electron impact, 70 eV): 276 (M^+) (Fig. S1).

Synthesis of Poly(DEAEMA-*co*-MMA-*co*-AntMac)

Poly(DEAEMA-*co*-MMA-*co*-AntMac) (PDMA) was prepared by free-radical polymerization (FRP) in the presence of AIBN under nitrogen atmosphere. To a flask equipped with a magnetic stirring bar, 0.5 mL of DMF, MMA (0.432 mL, 4.06 mmol), DEAEMA (0.153 mL, 0.75 mmol), AntMac (0.07 g, 0.25 mmol), and AIBN (0.0147 g, 0.09 mmol) were added in that order. After short nitrogen bubbling, the reaction flask was placed in a thermostated oil bath for 24 h at 85 °C. At the end of the period, solvent was evaporated and the resulting product was precipitated two times using THF as a good solvent and cold *n*-hexane as a poor solvent. Polymeric product was filtered and dried for 24 h at room temperature. Yield: 72%.

Synthesis of SCNP

Total of 150 mg of PDMA was dissolved in 300 mL of THF and the solution was stirred for 10 min under nitrogen bubbling and continued stirring for 120 min at room temperature under nitrogen atmosphere. Subsequently, solution was irradiated in a photoreactor consisting of 18 lamps at $\lambda_{(\text{nominally})}$ = 350 nm for 60 min. At the end of the irradiation period, solvent was evaporated and product was dried in a vacuum oven at room temperature.

Modification of SCNP with 1-(Bromoacetyl)pyrene

The Menschutkin reaction of SCNP was carried out with 1-(bromoacetyl)pyrene to synthesize the pyrene functionalized SCNPs in DMF. A typical quaternization was conducted as follows: SCNP (100 mg) was diluted in 2 mL of DMF. The mixture of 1-(bromoacetyl)pyrene (80 mg) and 1 mL of DMF was added dropwise into the prepared polymer solution. Under continuous stirring for 24 h, solvent was completely evaporated and solid polymer was dissolved in 3 mL of THF. Resulting polymer was precipitated in 50 mL of cold *n*-hexane. Solid copolymer was redissolved in THF and reprecipitated in cold *n*-hexane to remove unreacted 1-(bromoacetyl)pyrene. Then, polymer was filtered and dried in vacuum at 30 °C for 24 h. Yield: 45%.

Modification of MWCNT with SCNP-Py (SCNP-Py@MWCNT) and SCNP (SCNP@MWCNT)

Total of 40 mg of polymeric nanoparticle (SCNP or SCNP-Py) was dissolved in a round-bottom flask in 20 mL of THF and

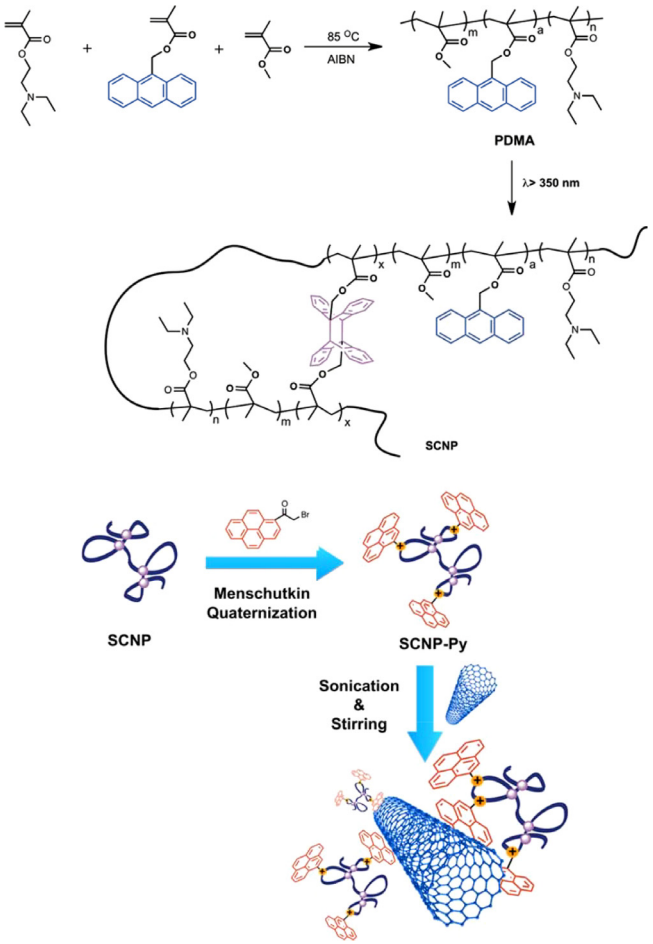

SCHEME 1 Overall synthetic mechanism for the SCNP-coated MWCNT. [Color figure can be viewed at wileyonlinelibrary.com]

30 mg CNT was added. The mixture was sonicated for 15 min in an ultrasonic bath and allowed to stir for 3 days. At the end of this period, the resulting mixture was filtered and washed with 80 mL fresh THF through Teflon membrane to eliminate the unattached polymeric nanoparticles. The final product was dried in vacuum at 30 °C for 24 h.

RESULTS AND DISCUSSION

In this study, we propose a new perspective to have dense polymeric coil obtained by folding process through intramolecular photodimerization onto CNT surface.

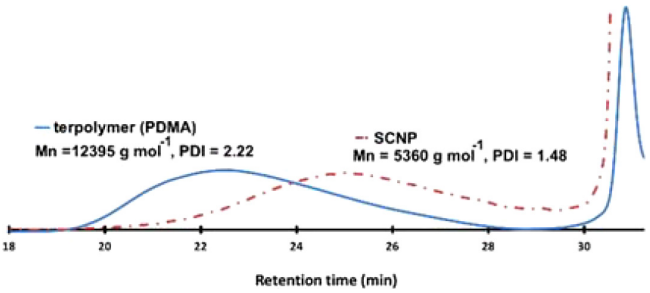

FIGURE 1 GPC traces of terpolymer (solid line) and SCNP (dash line) recorded with RI detector in THF at 35 °C. [Color figure can be viewed at wileyonlinelibrary.com]

In order to achieve anthracene and tertiary amine containing copolymer structure, MMA, 2-(diethylamino)ethyl methacrylate and AntMac were used in thermally initiated FRP (Scheme 1). Targeted linear copolymer consists of randomly distributed three different monomer groups. Side-chain anthracene moieties were utilized to form intramolecular crosslinked structure with photodimerization procedure and tertiary amine functionalities were subsequently quaternized by 1-(bromoacetyl)pyrene for the attachment onto CNT via noncovalent interactions (Scheme 1). According to ^{1}H NMR results of the PDMA, lateral protons of each monomer show that free-radical copolymerization was successfully performed. Ester protons (-OCH_2) of DEAEMA and AntMac appeared at 4.07 and 6.13 ppm, respectively. In addition, -OCH_3 protons of MMA were detected at 3.65 ppm and DEAEMA/MMA/AntMac compositions were in good agreement with monomer feed ratios using calculation of integral area of each segment (Fig. S2 and Table 1).

It is well known that SCNPs have more compact architectures and their molecular weight values are generally smaller than their precursors. Berda and coworkers successfully synthesized sub-20 nm soft nanoparticles using intramolecular photodimerization of pendant anthracene units.[12] According to the results of their work, high anthracene concentration in the copolymer causes unavoidable intermolecular crosslinking reactions. Therefore, we limited the concentration of AntMac monomer at 5% mol during the synthesis of terpolymer (PDMA). ^{1}H NMR results revealed that concentration of anthracene moieties in terpolymer and photodimerization degree of anthracene moieties in SCNP are 4 and 65%, respectively. After photodimerization process, molecular weight

TABLE 1 Copolymer Compositions, Molecular Weight Results, and Particle Size Comparisons of Terpolymer and Single-Chain Collapsed Nanoparticle

Sample	DEAEMA conc. in copolymer[b] (mol %)	AntMac conc. in copolymer[b] (mol %)	M_n[c] (g mol^{-1})	Polydispersity index[c]	Rh[d] (mm)
PDMA[a]	14	4	12395	2.22	7.4
SCNP	–	–	5360	1.48	5.2

[a] Feed ratio of DEAEMA/MMA/AntMac = (15/80/5 mol %).
[b] Calculated by ^{1}H NMR spectra.
[c] Determined by GPC according to linear PS standards.
[d] Particle size (nm) determined by DLS for nanoparticle samples suspended in THF.

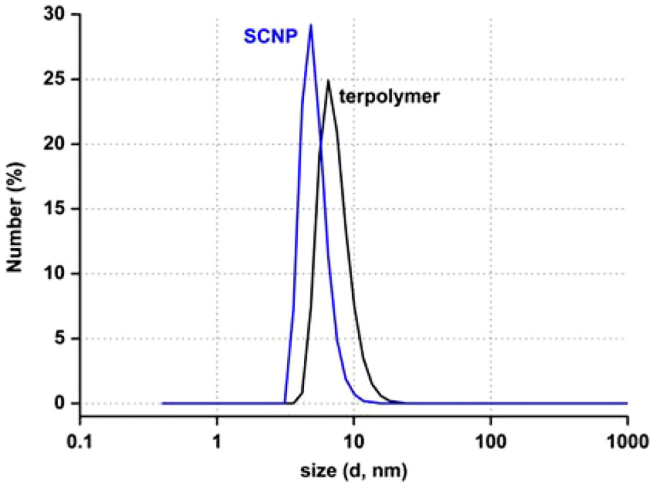

FIGURE 2 DLS measurements of PDMA (black line) and SCNP (blue line) at 25 °C in THF. [Color figure can be viewed at wileyonlinelibrary.com]

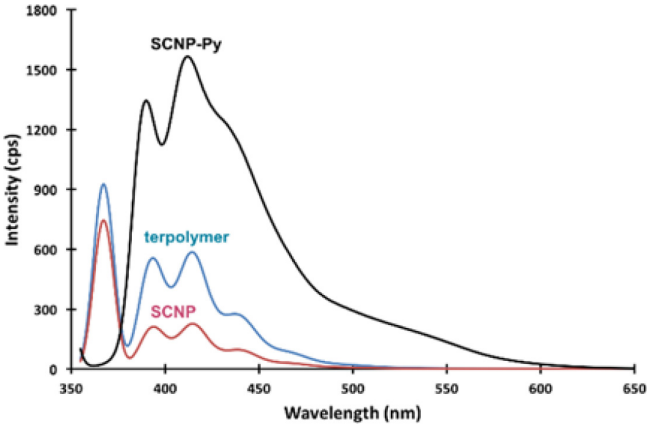

FIGURE 4 Emission spectra of terpolymer, SCNP, and SCNP-Py in THF ($c = 7 \times 10^{-4}$ mg mL^{-1}, λ_{exc} = 345 nm). [Color figure can be viewed at wileyonlinelibrary.com]

value of collapsed particle is quite different comparing to its noncrosslinked precursor as excepted (Table 1 and Fig. 1).

In addition, hydrodynamic radius of resulting nanoparticle decreases because obtained nanoparticle has much more compact size than its linear precursor (Fig. 2 and Table 1).

As can be seen from both UV–visible (UV–vis) and fluorescence spectra, after light-induced dimerization of anthracene moieties, absorption, and fluorescence intensity values decrease (Figs. 3 and 4). Besides, pyrene-modified SCNP sample exhibit very high intensity in emission spectra between 365 and 600 nm due to the high quantum yield of pyrene moieties (Fig. 4). Moreover, side-chain anthracene functionalities still exist in the SCNP and they are easily detectable by spectral analyses.

Thermal properties of terpolymer and SCNP were also investigated by DSC analyses. Intramolecular crosslinked nanoparticles (SCNP) have higher *Tg* value compared to linear copolymer precursor. Reduced chain mobility of the nanoparticle resulted by intramolecular photodimerization causes a significant increase in glass transition temperature (*Tg*) which shifts from 98.71 to 130.52 °C (Fig. 5). Also, it was previously reported that heating the dimer product between 160 and 200 °C temperatures causes to scission into its corresponding anthracene moieties.[35,36] Therefore, we did not exceed 160 °C during analyses in order to avoid scission of dimerized junction points along the copolymer structure.

In order to gain more insight into thermal behavior of nanoparticle decorated MWCNT and pyrene analogue of SCNP, TGAs were carried out as well (Fig. 6). Pyrene-modified

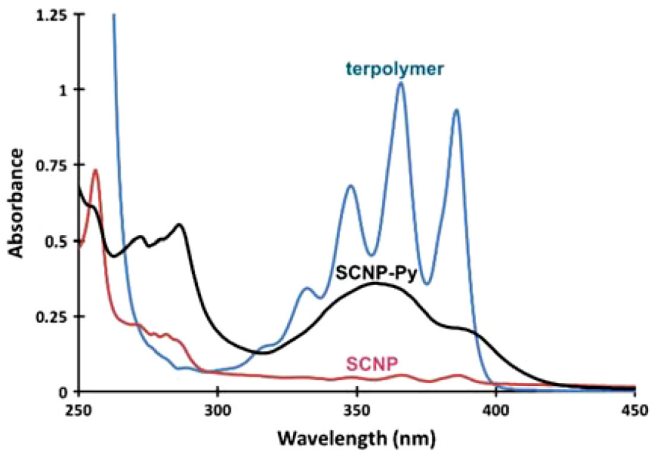

FIGURE 3 Absorption spectra of terpolymer, SCNP, and SCNP-Py in THF ($c = 2 \times 10^{-1}$ mg mL^{-1}). [Color figure can be viewed at wileyonlinelibrary.com]

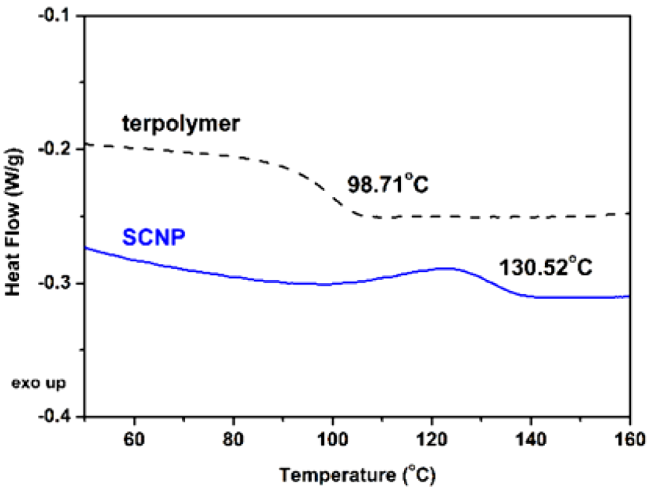

FIGURE 5 DSC thermograms (second heating scan) of terpolymer and SCNP. [Color figure can be viewed at wileyonlinelibrary.com]

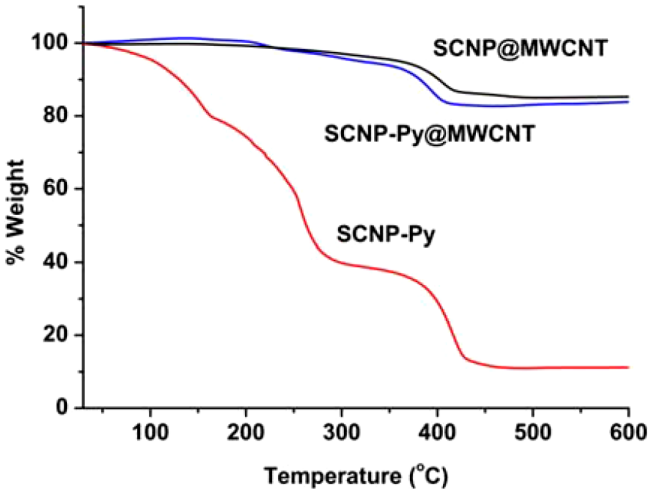

FIGURE 6 Thermogravimetric analyses of SCNP-Py, SCNP-Py@MWCNT, and SCNP@MWCNT. [Color figure can be viewed at wileyonlinelibrary.com]

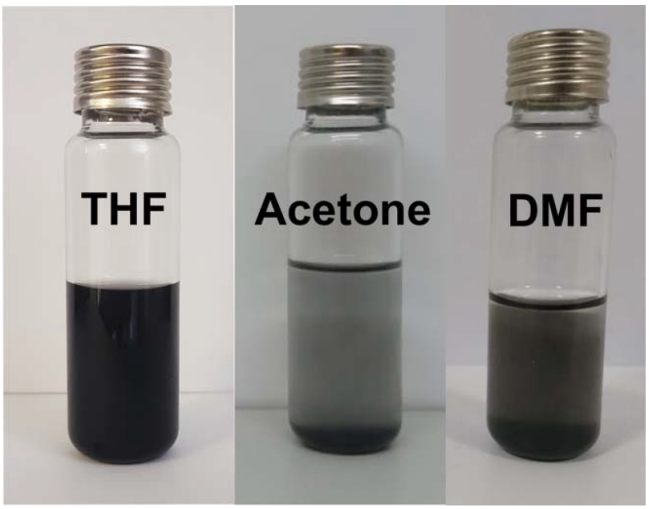

FIGURE 7 Durability images of SCNP-Py@MWCNT in different solvents. [Color figure can be viewed at wileyonlinelibrary.com]

polymeric nanoparticle has a char yield (12%) because of ionic moieties and rigid dangling pyrene groups in the structure. MWCNT was also modified with SCNPs in order to compare grafting ratios of SCNP and SCNP-Py. While SCNP-Py coated MWCNT sample shows 18% grafting ratio, SCNP@MWCNT sample has 14% polymer content according to TGA results. These results show that pyrene existence in the nanoparticle architecture increases grafting ratio of SCNP onto MWCNT's surfaces as expected. On the other hand, due to the existence of bare anthracene units on folded nanoparticles, noncovalent interactions between anthracene groups and MWCNT's surface increase grafting ratio.

SCNP-Py@MWCNT samples in different solvents were demonstrated in Figure 7 to determine the dispersion properties. After sonication, samples exhibit poor dispersion behavior in acetone and DMF in 15 min. Even though THF shows better solubility than DMF and acetone, particle aggregation was detected after 1 h. This particle association was ascribed to increase interconnection tendency of CNT particles by pyrene functionalized folding nanoparticles.

Although DLS measurement of SCNP emphasizes sub-10 nm particle size, TEM pictures demonstrate that polymeric nanoparticles tend to be larger globular shape due to the chain aggregation (Fig. S3). This trend can be explained by solvent evaporation after casting on a copper grid; therefore, particles seem to incline to association during drying. TEM photographs of SCNP-Py-modified CNTs exhibit large aggregation behavior and this manner may be attributed to high interaction capability of SCNPs possessing pyrene groups with different MWCNT surfaces [Fig. 8(A)]. In higher magnifications, sub-10 nm sized globular shaped polymeric nanoparticles are obviously seen on CNT particles and this attitude makes pyrene containing SCNPs potential crossing points for CNT particles [Fig. 8(B,C)].

CONCLUSIONS

In conclusion, we have demonstrated the decoration of polymeric nanoparticles onto CNT surface via noncovalent interactions. Polymeric nanoparticles have been produced by photodimerization process of anthracene species on the side chain of the linear terpolymer. GPC, DLS, and TEM results revealed that single-chain polymeric nanoparticles were successfully synthesized. Next, pyrene moieties were incorporated into the tertiary amine pendant groups of polymeric nanostructure using straightforward quaternization reaction. According to UV–vis and fluorescence spectra, SCNP production and its pyrene functionalization were successfully carried out. Pyrene containing SCNPs were grafted onto MWCNT side walls by π–π stacking strategy. Incorporated pyrene units were strongly interacted with MWCNT surfaces as was evidenced by TGA results and electron microscopy studies. Electron microscopy images showed polymeric particles

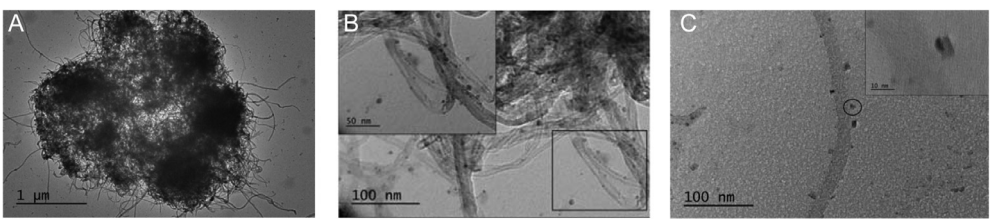

FIGURE 8 HRTEM images of SCNP-Py@MWCNT.

interconnect to MWCNTs and contribute the particle aggregation. We assume that this route will bring a new perspective to achieve hybrid nanomaterials. Moreover, waste and stable CNT particles in organic solvents can be collected by SCNPs using straightforward noncovalent strategy.

REFERENCES AND NOTES

1 W. Fan, X. Tong, F. Farnia, B. Yu, Y. Zhao, *Chem. Mater.* **2017**, *29*, 5693.

2 H. Rothfuss, N. D. Knöfel, P. W. Roesky, C. Barner-Kowollik, *J. Am. Chem. Soc.* **2018**, *140*, 5875.

3 J. Rubio-Cervilla, E. González, J. Pomposo, *Nanomaterials* **2017**, *7*, 341.

4 R. Lambert, A.-L. Wirotius, D. Taton, *ACS Macro Lett.* **2017**, *6*, 489.

5 C.-C. Cheng, D.-J. Lee, Z.-S. Liao, J.-J. Huang, *Polym. Chem.* **2016**, *7*, 6164.

6 N. Ormategui, I. Garcia, D. Padro, G. Cabanero, H. J. Grande, I. Loinaz, *Soft Matter* **2012**, *8*, 734.

7 C. Heiler, S. Bastian, P. Lederhose, J. P. Blinco, E. Blasco, C. Barner-Kowollik, *Chem. Commun.* **2018**, *54*, 3476.

8 S. Babaoglu, D. Karaca Balta, G. Temel, *J. Polym. Sci. Part A: Polym. Chem.* **2017**, *55*, 1998.

9 A. Ruiz de Luzuriaga, N. Ormategui, H. J. Grande, I. Odriozola, J. A. Pomposo, I. Loinaz, *Macromol. Rapid Commun.* **2008**, *29*, 1156.

10 H. Cengiz, B. Aydogan, S. Ates, E. Acikalin, Y. Yagci, *Des. Monomers Polym.* **2011**, *14*, 69.

11 A. Sanchez-Sanchez, I. Asenjo-Sanz, L. Buruaga, J. A. Pomposo, *Macromol. Rapid Commun.* **2012**, *33*, 1262.

12 P. G. Frank, B. T. Tuten, A. Prasher, D. Chao, E. B. Berda, *Macromol. Rapid Commun.* **2014**, *35*, 249.

13 J. He, L. Tremblay, S. Lacelle, Y. Zhao, *Soft Matter* **2011**, *7*, 2380.

14 K. N. R. Wuest, H. Lu, D. S. Thomas, A. S. Goldmann, M. H. Stenzel, C. Barner-Kowollik, *ACS Macro Lett.* **2017**, *6*, 1168.

15 T. Mes, R. van der Weegen, A. R. A. Palmans, E. W. Meijer, *Angew. Chem. Int. Ed.* **2011**, *50*, 5085.

16 E. Harth, B. Van Horn, V. Y. Lee, D. S. Germack, C. P. Gonzales, R. D. Miller, C. J. Hawker, *J. Am. Chem. Soc.* **2002**, *124*, 8653.

17 J. Xiaotian, Z. Yue, Z. Hanying, *Chem. Eur. J.* **2018**, *24*, 3005.

18 A. M. Hanlon, R. Chen, K. J. Rodriguez, C. Willis, J. G. Dickinson, M. Cashman, E. B. Berda, *Macromolecules* **2017**, *50*, 2996.

19 W. Zhang, Z. Zhang, Y. Zhang, *Nanoscale Res. Lett.* **2011**, *6*, 55.

20 C. M. Tan, C. Baudot, Y. Han, H. Jing, *Nanoscale Res. Lett.* **2012**, *7*, 183.

21 F. Kreupl, A. P. Graham, G. S. Duesberg, W. Steinhögl, M. Liebau, E. Unger, W. Hönlein, *Microelectron. Eng.* **2002**, *64*, 399.

22 L. Sun, X. Wang, Y. Wang, Q. Zhang, *Carbon* **2017**, *122*, 462.

23 E. Bekyarova, Y. Ni, E. B. Malarkey, V. Montana, J. L. McWilliams, R. C. Haddon, V. Parpura, *J. Biomed. Nanotechnol.* **2005**, *1*, 3.

24 Y.-P. Sun, K. Fu, Y. Lin, W. Huang, *Acc. Chem. Res.* **2002**, *35*, 1096.

25 H. Durmaz, A. Dag, U. Tunca, G. Hizal, *J. Polym. Sci. Part A: Polym. Chem.* **2012**, *50*, 2406.

26 O. Zabihi, M. Ahmadi, M. Akhlaghi bagherjeri, M. Naebe, *RSC Adv.* **2015**, *5*, 98692.

27 G. Temel, M. Uygun, N. Arsu, *Polym. Bull.* **2013**, *70*, 3563.

28 G. Sakellariou, D. Priftis, D. Baskaran, *Chem. Soc. Rev.* **2013**, *42*, 677.

29 C. Gao, W. Li, H. Morimoto, Y. Nagaoka, T. Maekawa, *J. Phys. Chem. B* **2006**, *110*, 7213.

30 M. Un, G. Temel, *Eur. Polym. J.* **2018**, *105*, 398.

31 P. D. Petrov, G. L. Georgiev, A. H. E. Müller, *Polymer* **2012**, *53*, 5502.

32 L. Lei, K. C. Etika, K. S. Liao, L. A. Hess, D. E. Bergbreiter, J. C. Grunlan, *Macromol. Rapid Commun.* **2009**, *30*, 627.

33 T. Yutaka, T. Mitsuhiro, S. Yuuki, Y. Yasushi, T. Sadao, U. Tetsuya, S. Kaoru, K. Shin-ichi, W. Takatsugu, M. Yutaka, A. Takeshi, *Chem. Lett.* **2005**, *34*, 1608.

34 X. Lou, R. Daussin, S. Cuenot, A.-S. Duwez, C. Pagnoulle, C. Detrembleur, C. Bailly, R. Jérôme, *Chem. Mater.* **2004**, *16*, 4005.

35 J. Van Damme, O. van den Berg, J. Brancart, L. Vlaminck, C. Huyck, G. Van Assche, B. Van Mele, F. Du Prez, *Macromolecules* **2017**, *50*, 1930.

36 J. Van Damme, L. Vlaminck, G. Van Assche, B. Van Mele, O. van den Berg, F. Du Prez, *Tetrahedron* **2016**, *72*, 4303.